

Supplemental materials

- 1 PART-1. Long-term nor-NOHA treatment in chronic-onset PKD mice**
- 2 PART-2. ARG1 stimulates CLEC proliferation as a free cytokine**
- 3 Supplemental figures and legends**

PART-1. Long-term nor-NOHA treatment in chronic-onset PKD mice (Fig. S8)

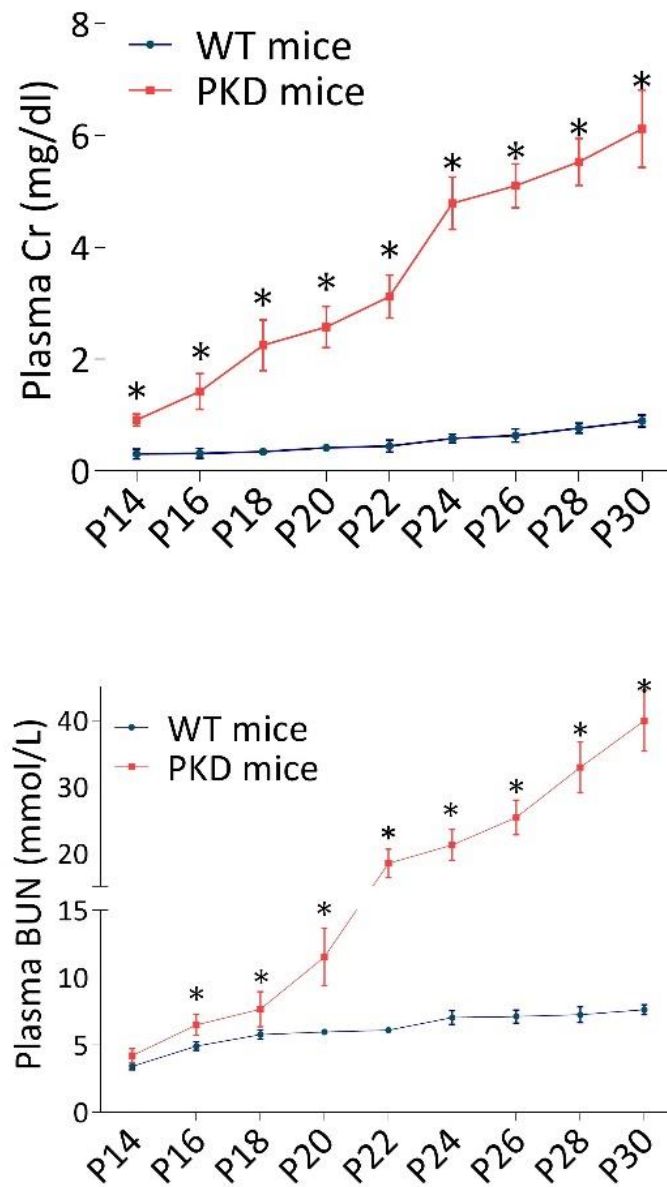
Briefly, the *Pkd1* gene was inactivated in mice at P30 and microcyst formation was observed in the kidneys at approximately P180. Chronic-onset PKD mice were treated with nor-NOHA for 4 months during P180–P300; volume-matched normal saline solution (NS) was administered to age/weight-matched PKD mice via intraperitoneal injection as a control. Four months of nor-NOHA treatment significantly improved the general survival rates, postponed cyst growth, lowered the CIs, protected renal functions, and inhibited cell proliferation. Compared to short-term (P14–P32) nor-NOHA treatment in rapid-onset PKD mice, 4 months of treatment significantly inhibited the production of L-lactic acid and downregulated the expression of ARG1 in chronic-onset polycystic kidneys. Downregulation of ARG1 and inactivation of arginase activity significantly inhibited the arginine-polyamine metabolic pathway and promoted nitric oxide (NO) generation in polycystic kidney tissue.

PART-2. ARG1 stimulates CLEC proliferation as a free cytokine (Fig. S9)

Significantly higher levels of ARG1 were detected in DMEM from L-LA-induced RAW264.7 cells and urine samples from ADPKD patients compared to respective controls. Further, ARG1 significantly increased the populations of CLECs in the S stage and promoted the incorporation of EdU into their DNA. The expression of phosphorylated-ERK 1/2 was significantly upregulated in ARG1-treated CLECs; therefore, the pro-proliferative function of ARG1 in CLECs might be achieved by activating the ERK pathway. Because nor-NOHA failed to offset the effects of ARG1 on CLECs, ARG1 might influence CLEC proliferation via a pathway independent of arginine-polyamine metabolism.

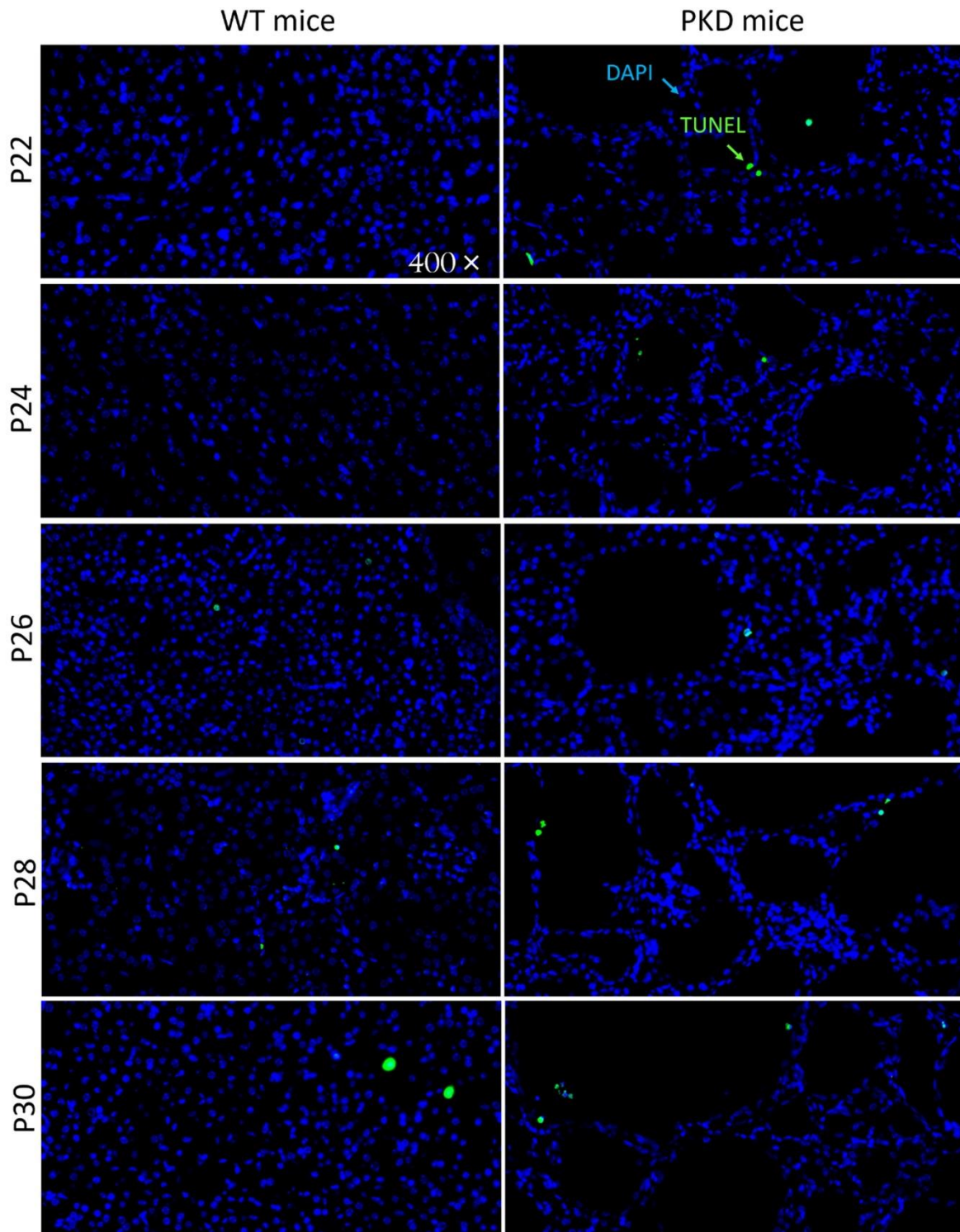
Supplement Figures

Fig. S1. Renal function in rapid-onset PKD mice



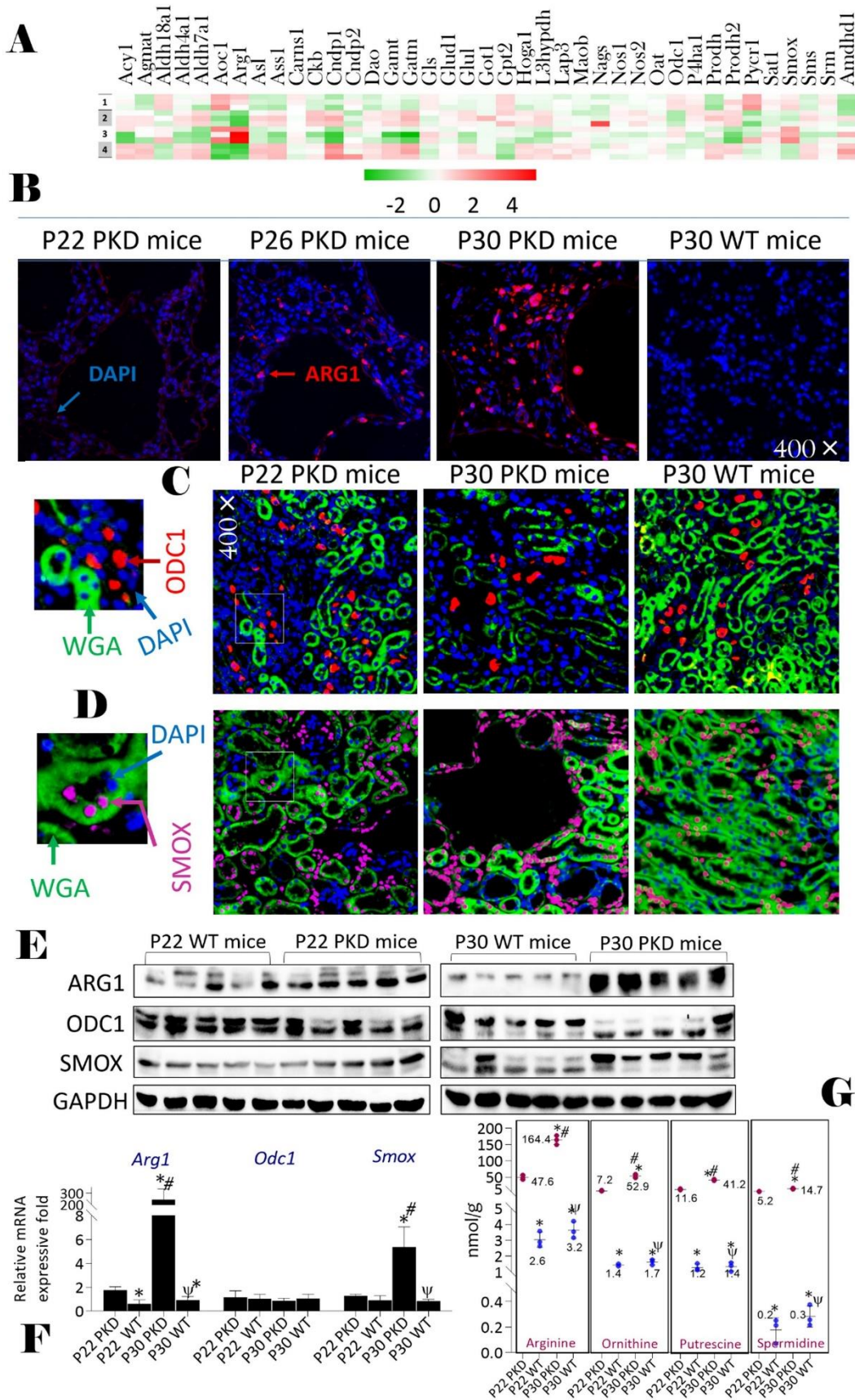
Renal function deteriorated progressively with postnatal age. * $p < 0.05$ vs. age-matched WT littermates. Data are presented as means \pm SDs, with 5–6 PKD and age-matched WT mice at different postnatal ages.

Fig. S2. Apoptotic cells in polycystic kidneys



TUNEL-labeled nuclei (green) were counted in polycystic kidneys at different postnatal ages, 400×. DAPI (blue) was used to illuminate the nuclei. * $p < 0.05$ v. age-matched polycystic kidneys. Data are presented as means \pm SDs, with five PKD mice each at P22, P26, P26, P28, and P30.

Fig. S3. Activation of arginine-polyamine metabolism in polycystic kidneys

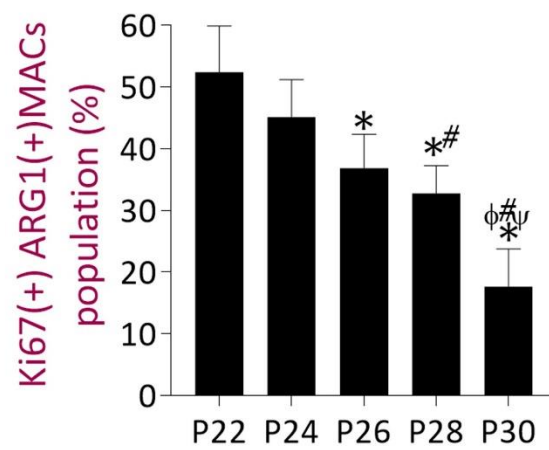
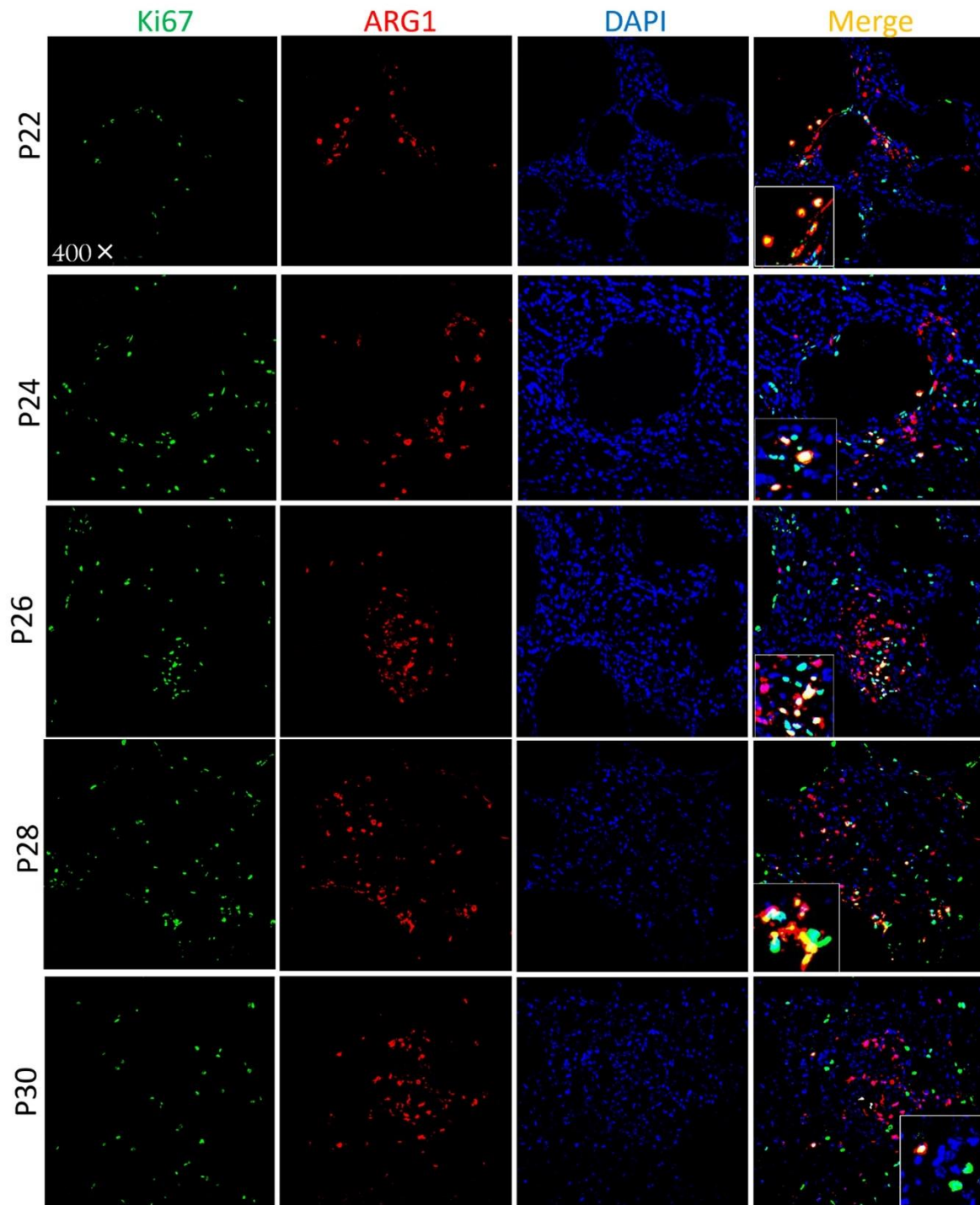


(A) mRNA expression profiles of genes encoding proteins involved in the arginine-polyamine metabolic pathway: 1, P22 polycystic kidneys; 2, P22 WT kidneys; 3, P30

polycystic kidneys; 4, P30 WT kidneys. (B–D) Tissue localization of ARG1, ODC1, and SMOX in polycystic kidney sections by IHC or fluorescence-IHC. (B) ARG1 (red) was located in the renal interstitium, 400×. DAPI (blue) was used to illuminate the nuclei. (C) WGA (green), ODC1 (red), and DAPI (blue) were co-stained in polycystic kidney sections at P22 and P30, 400×. Autofluorescence (WGA, green) was used to illuminate the tubular structures. Most ODC1-stained cells were located in the renal interstitium. (D) WGA (green), SMOX (red), and DAPI (blue) were co-stained in polycystic kidney sections at P22 and P30, 400×. (E, F) mRNA and protein expression in polycystic kidneys compared to WT kidneys at P22 and P30, respectively. (G) L-arginine, L-ornithine, putrescine, and spermidine levels in polycystic kidneys compared to WT kidneys at P22 and P30, respectively; the mean value of each metabolite is labeled. * $p < 0.05$ vs. P22 polycystic kidneys; # $p < 0.05$ vs. P22 WT kidneys; $^{\psi}p < 0.05$ vs. P30 polycystic kidneys. Data are presented as means \pm SDs, with five or six PKD and WT mice at P22 and P30, respectively.

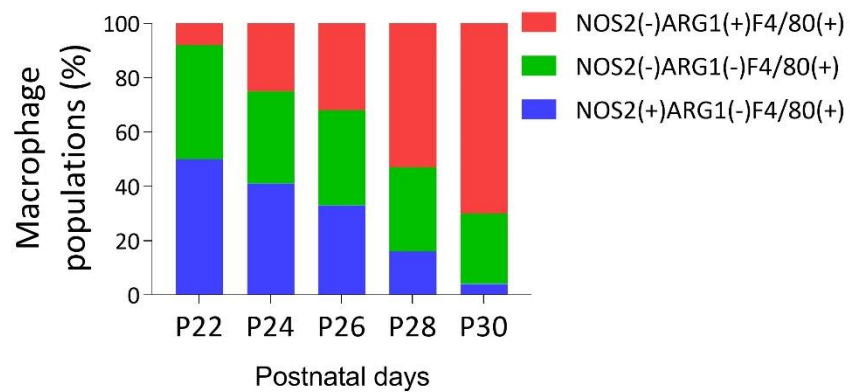
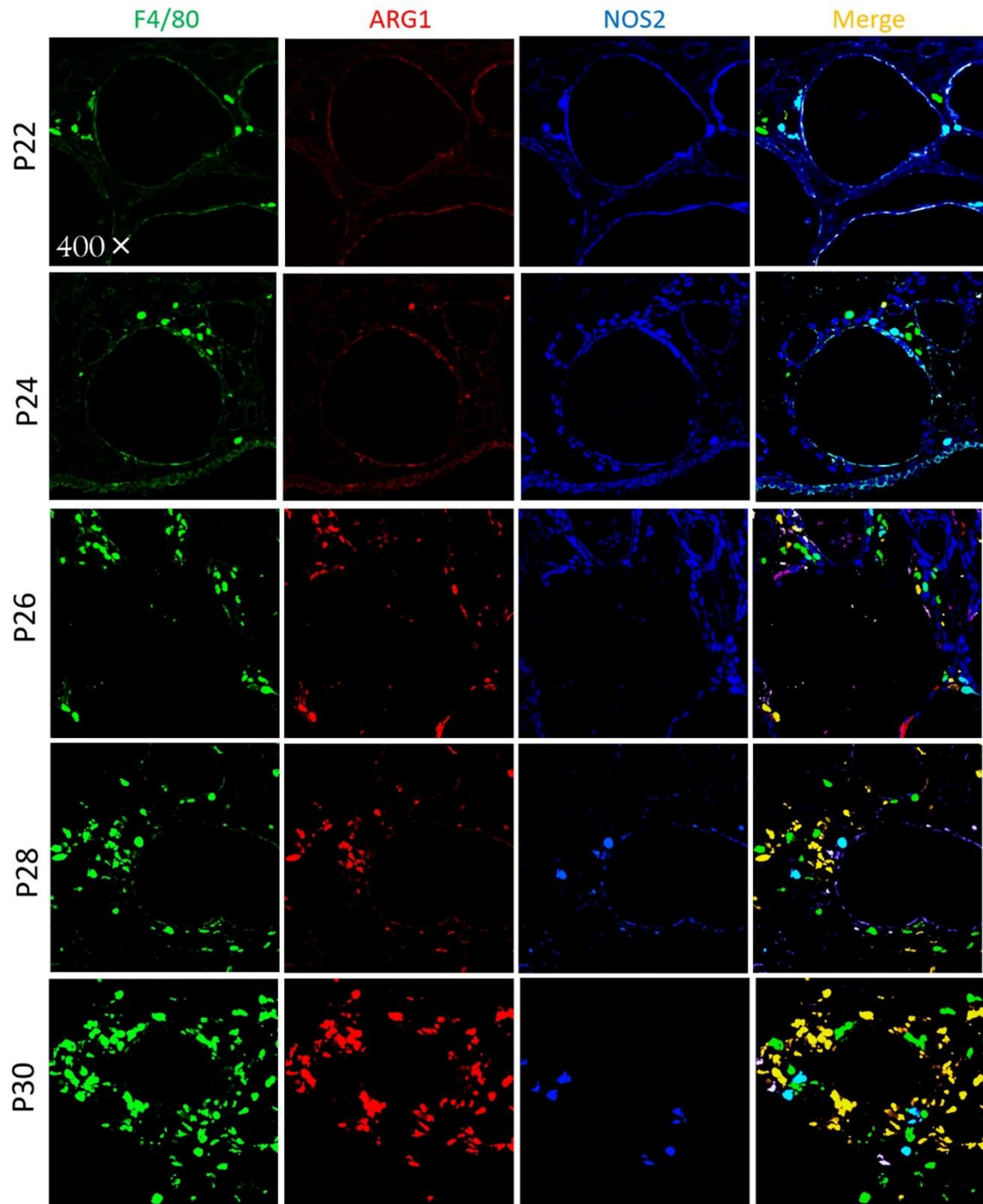
In all, 204 DEGs are summarized. Their expressions were compared among P22 polycystic, P22 WT, P30 polycystic, and P30 WT kidneys. Data are presented as means \pm SDs, with three PKD and WT mice at P22 and P30, respectively. *Arg1* is shown with a red arrow.

Fig. S5. Proliferating ARG1 (+) macrophages in polycystic kidneys



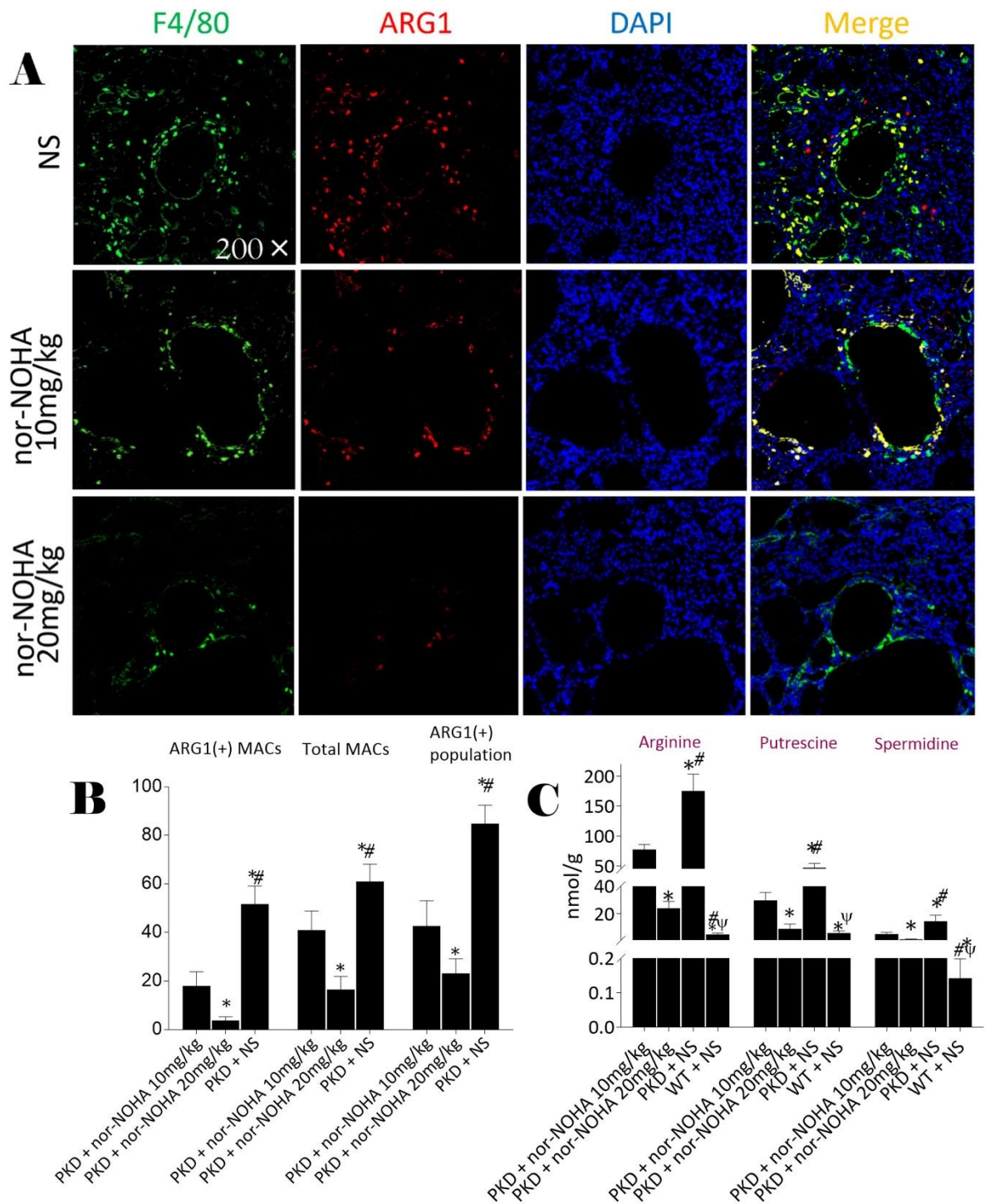
Co-staining with ARG1 (red), Ki-67 (green), and DAPI (blue) in polycystic kidneys at postnatal ages P22–P30, 400 \times . * $p < 0.05$ vs. P22 polycystic kidneys; # $p < 0.05$ vs. P24 polycystic kidneys; $\psi p < 0.05$ vs. P26 polycystic kidneys; $\phi p < 0.05$ vs. P28 polycystic kidneys. Data are presented as means \pm SDs, with five or six mice at different postnatal ages.

Fig. S6. Transition of macrophage populations in polycystic kidneys



F4/80 (green), NOS2 (blue), and ARG1 (red) were co-localized in polycystic kidneys at P22, P24, P26, P28, and P30, 400 \times . Data are presented as means \pm SDs, with 5–6 PKD mice at different postnatal ages.

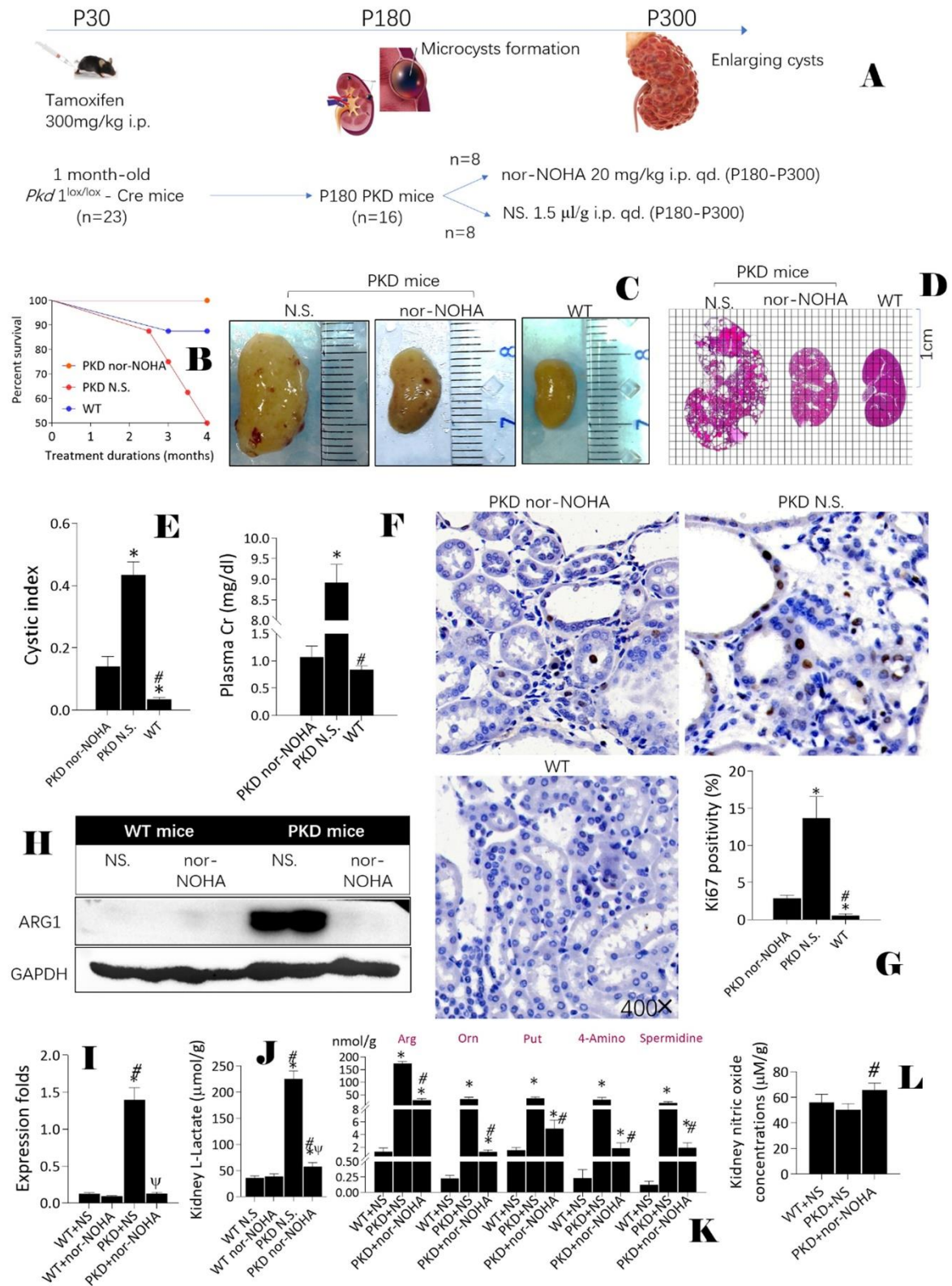
Fig. S7. Nor-HOHA treatment in rapid-onset PKD mice



(A, B) ARG1 (+) macrophage counts in polycystic kidneys were compared among PKD mice treated with different doses of nor-NOHA, 200×. (C) Nor-NOHA remarkably inhibited polyamine synthesis in polycystic kidneys. * $p < 0.05$ vs. 10 mg/kg nor-NOHA-treated PKD mice; # $p < 0.05$ vs. 20 mg/kg nor-NOHA-treated PKD mice; $\psi p < 0.05$ vs. NS-treated PKD

mice. Data are presented as means \pm SDs, with 4–6 mice receiving different doses of nor-
NOHA.

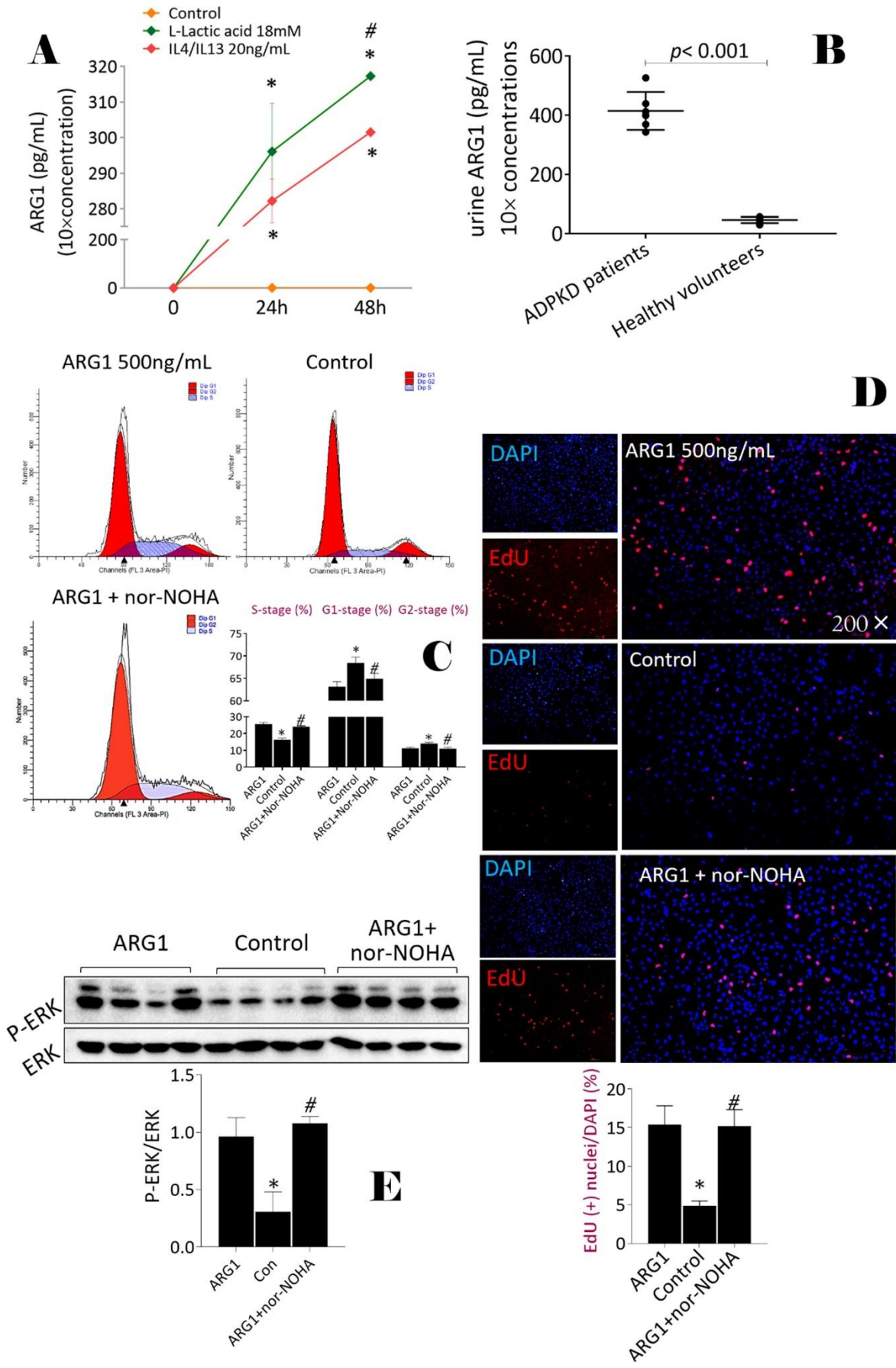
Fig. S8. Nor-NOHA treatment in chronic-onset PKD mice



(A) Generation of chronic-onset PKD mice and providing 4-month nor-NOHA intervention in the model. Sixteen PKD mice at P180 were randomized into two groups: one group received nor-NOHA 20 mg/kg, qd., i.p. and the other group received normal saline (NS) 1.5

$\mu\text{L/g}$, qd., i.p. All mice were sacrificed at P300. (B–F) Comparison of the general survival rates (B), gross kidney appearance (C), cystic indices (D, E), and renal functions (F) among nor-NOHA-treated PKD mice, NS-treated PKD mice, and NS-treated WT mice. $*p < 0.05$ vs. nor-NOHA-treated PKD mice; $\#p < 0.05$ vs. NS-treated PKD mice. (G) The renal proliferation rates were compared among three groups using Ki-67 IHC staining, 400 \times . $*p < 0.05$ vs. nor-NOHA-treated PKD mice; $\#p < 0.05$ vs. NS-treated PKD mice. (H–J) The expression of ARG1 (H, I) and L-lactic acid (J) in kidney tissues was detected in nor-NOHA-treated PKD mice, NS-treated PKD mice, nor-NOHA-treated WT mice, and NS-treated WT mice. $*p < 0.05$ vs. NS-treated WT mice; $\#p < 0.05$ vs. nor-NOHA-treated WT mice; $\psi p < 0.05$ vs. NS-treated PKD mice. (K, L) Arginine-polyamine metabolites (K) and nitric oxide (L) in kidney tissues were assayed and compared among nor-NOHA-treated PKD mice, NS-treated PKD mice, and NS-treated WT mice. Arg, arginine; Orn, ornithine; Put, putrescine; 4-Amino, 4-aminobutyraldehyde; NO, nitric oxide. $*p < 0.05$ vs. NS-treated WT mice; $\#p < 0.05$ vs. NS-treated PKD mice. Data are presented as means \pm SDs, with 4–8 PKD mice or age-matched WT mice.

Fig. S9. Pro-proliferative function of ARG1 as a free cytokine



(A) The levels of ARG1 were assayed in DMEM from L-LA-treated RAW264.7 cells, IL4/IL-13-treated RAW264.7 cells, and control cells. $*p < 0.05$ vs. control; $\#p < 0.05$ vs. IL4/IL13-treated RAW264.7 cells. (B) ARG1 secretion in urine specimens was compared between ADPKD patients and healthy volunteers. (C) Cell cycle analyses of ARG1-treated and ARG1 + nor-NOHA-treated CLECs was performed using a flow cytometer. (D) 5-Ethynyl-2'-deoxyuridine (EdU, red) nuclei staining was used to compare the proliferation rates of CLECs, 200 \times . All nuclei were stained with DAPI (blue). (E) The expression of phosphorylated-ERK 1/2 was compared among ARG1-treated CLECs, ARG1 + nor-NOHA-treated CLECs, and control. $*p < 0.05$ vs. ARG1-treated CLECs; $\#p < 0.05$ vs. control. Data are presented as means \pm SDs, with four cell specimens from different treatments.